Available online at www.sciencedirect.com
SCIENCE DIRECT®
Journal of Crystal Growth 282 (2005) 383–388
JOURNAL OF CRYSTAL GROWTH
www.elsevier.com/locate/jcrysgro

In situ synthesis and phase transformation of In_2O_3/Sb core-shell nanostructures

C.W. Lai[a], J.Y. Dai[a,*], X.Y. Zhang[a], H.L.W. Chan[a], Y.M. Xu[b], Quan Li[b], H.C. Ong[b]

[a]*Department of Applied Physics and Materials Research Center, The Hong Kong Polytechnic University, Hung Hom, Kowloon, Hong Kong, PR China*
[b]*Department of Physics, The Chinese University of Hong Kong, Shatin, New territory, Hong Kong, PR China*

Received 24 March 2005; accepted 9 May 2005
Available online 28 June 2005
Communicated by R. Kern

Abstract

A simple low-temperature thermal evaporation method was utilized for a large-scale synthesis of In_2O_3/Sb core-shell cable-like nanostructures by co-evaporating In and Sb. An X-ray diffraction, transmission electron microscopy, and electron energy loss spectroscopy study revealed the formation of In_2O_3 nanowires at 540 °C with unique structures of rectangular turning and a co-axis structure with an amorphous Sb shell layer surrounding the In_2O_3 wires. The amorphous Sb layer was found to undergo a crystallization phase transition under a 200 keV focused electron beam irradiation. An epitaxial relationship was found to exist between the crystallized Sb and In_2O_3.

PACS: 61.46

Keywords: A1. Nanostructures; A1. Nanowire; A3. Physical vapor deposition process; A3. In_2O_3; A3. Core-shell structure

1. Introduction

One-dimensional nanostructured materials, such as nanowires, nanotubes, and nanobelts have drawn much attention due to their unusual properties and potential applications in optical and electronic devices [1–4]. As the development of nanoscale electronics approaches a practical stage, it is essential to assemble known functional materials in a radial direction within a single nanoscale building block to form heterostructures, namely coaxial nanocables. Nanocables can exhibit novel functional properties compared to the individual materials that constitute them. Thus far, many studies have focused on semiconductor core nanoscale heterostructures [5–7]. In_2O_3 is an

*Corresponding author. Tel.: 852 27664028; fax: 852 23337629.
E-mail address: apdaijy@inet.polyu.edu.hk (J.Y. Dai).

0022-0248/$ - see front matter © 2005 Elsevier B.V. All rights reserved.
doi:10.1016/j.jcrysgro.2005.05.026

important transparent semiconducting oxide material with a wide direct bandgap (3.6 eV) that has been widely used in solar cells, organic light-emitting diodes, and gas sensors. In_2O_3 nanowire can exhibit better sensitivity than the bulk due to enhanced surface-to-volume ratio, leading to improvements in the performance of sensors [8,9]. The performance of field effect transistors utilizing In_2O_3 nanowires is also expected to improve greatly [10,11].

In_2O_3 nanowires and other nanostructures have been synthesized by several techniques, such as the thermal evaporation method [12–16] and the carbothermal reduction method [17,18]. An ordered In_2O_3 nanowires array was synthesized by the oxidation of indium metal embedded by electrodeposition in anodic alumina membranes [19,20]. The diameter-controlled growth of the In_2O_3 nanowires was also achieved on Si/SiO_2 substrate covered with Au film as a catalyst using the laser ablation of the InAs target [10]. These methods generally require high temperatures and complicate steps. On the other hand, manipulating the nanowires into position and providing electrical contacts pose a challenge because of their small dimensions. In this letter, a novel low-temperature thermal evaporation growth method was developed for in situ growing of a core-shell structure of single crystalline In_2O_3 nanowire with an amorphous Sb sheath. The amorphous Sb sheath was found to undergo a crystallization phase transition under a 200 keV focused electron beam irradiation. The morphology, composition profiles, and growth mechanism of the nanostructures were also discussed.

2. Experimental procedure

The In_2O_3/Sb nanowires were synthesized by simple physical vapor deposition method. The mixture of indium granulars (99.999% purity) with a diameter of 1–3 mm and a small amount of antimony metal powder (98% purity) was positioned at the center of an alumina tube with a diameter of 6 cm and a length of 80 cm. Before heating, the alumina tube was filled with nitrogen gas with a flow rate of 200 sccm. The temperature of the furnace was increased from room temperature to 540 °C with a heating rate of 25 °C/min, and the furnace was kept at this temperature for 6–10 h. After the system was cooled down to room temperature, a black wool-like product was observed on the surface of indium granulars. The crystal structure of the product was identified by X-ray powder diffraction (XRD). The morphology and the composition of the products were examined by scanning electron microscopy (SEM). The structure and composition of the products were investigated by transmission electron microscopy (TEM) with a field emission gun operated at 200 keV and equipped with an energy dispersive X-ray (EDX) detector and with an electron energy loss spectroscopy (ELLS) analyzer.

3. Results and discussion

Fig. 1 shows the in situ SEM images of the wool-like product, revealing a formation of nanowires on a mass scale. It is apparent that the nanowires present a rectangular turning feature, and their diameter ranges from a few tens of nanometers to a few hundreds of nanometers, with a length of 10 μm and more. Fig. 2 depicts the corresponding XRD spectrum. The reflection peaks of the body-centered cubic structured In_2O_3 are distinguishable, and can be indexed to the In_2O_3 crystal structure with a lattice constant of $a = 1.012$ nm.

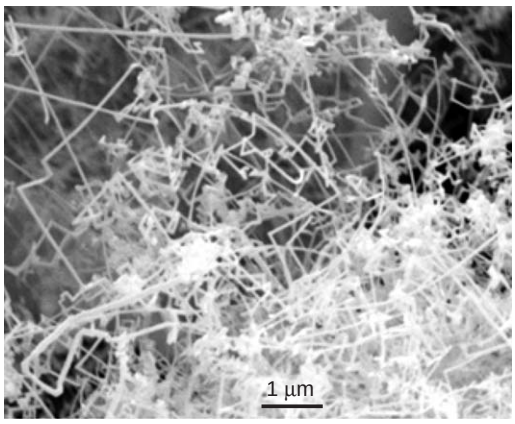

Fig. 1. SEM image of the as-synthesized a wool-like product.

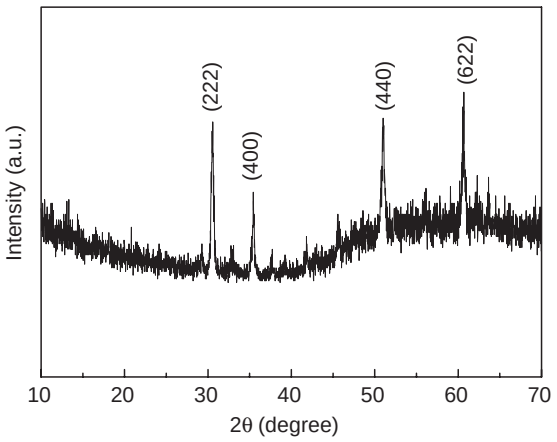

Fig. 2. XRD pattern of the as-synthesized product.

We further investigated the morphology, structure, and composition of the synthesized product by TEM, EDX, and EELS analysis. Fig. 3 shows the low-magnification TEM images of the nanowires. A selected-area electron diffraction (SAED) pattern from one of the nanowires could be indexed as a single-crystal cubic structured In_2O_3, with the growth direction along $\langle 1\,0\,0\rangle$. The In_2O_3 nanowires present typical morphologies of "L," "T," and "H" shapes as shown in Figs. 3(c) and (d). In these structures, the turning directions are identified as being consistently along the $\langle 1\,0\,0\rangle$ directions with a rectangular turning angle. The easily 90° turning of the In_2O_3 nanowires is due to the easy growth direction of $\langle 1\,0\,0\rangle$ of the cubic structure of In_2O_3. It is worth

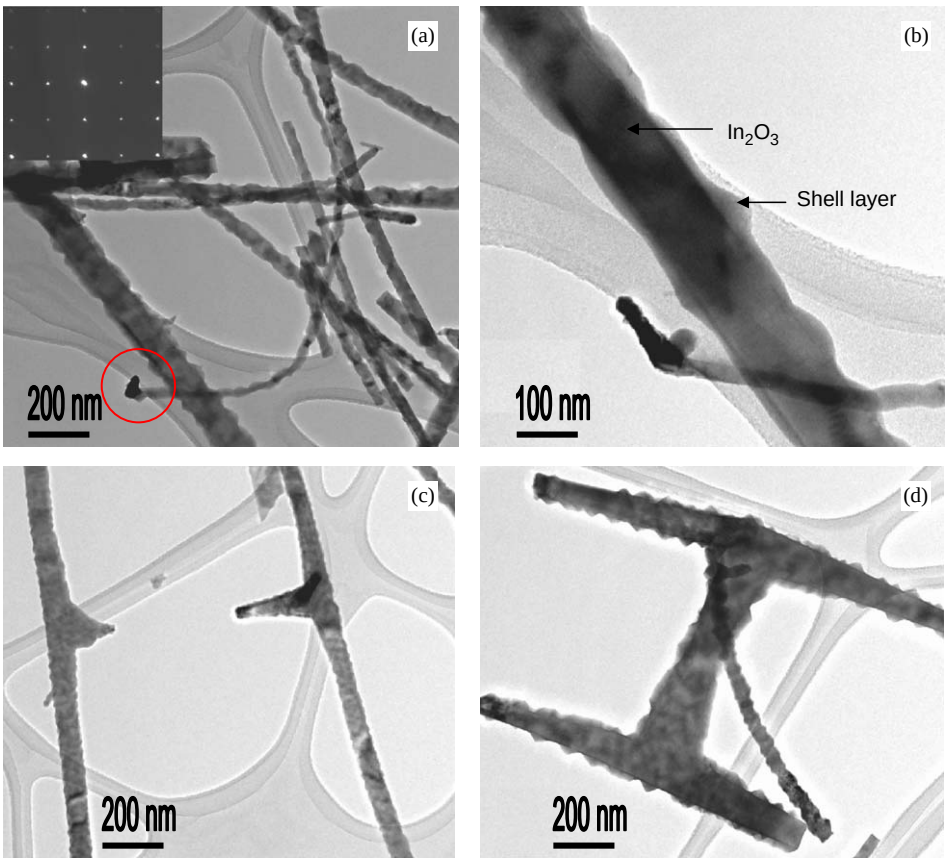

Fig. 3. (a) Typical low-magnification TEM image of the In_2O_3 nanowires; the inset shows the selected area electron diffraction pattern; (b) enlarged image of the circled area in (a) (c); "T"-shaped In_2O_3 nanowires; and (d) "H"-shaped In_2O_3 nanowires.

noting that the In_2O_3 nanowires exhibit a rough surface. As shown in Fig. 3(b), a shell layer around the In_2O_3 nanowires can be seen forming a co-axis structure. Careful observation by TEM revealed that some In_2O_3 nanowires contain a head with darker contrast, as indicated by a circle in Fig. 3(a). A nano-sized electron beam EDX analysis showed that the tip contains mainly Sb with less amount of In and O. A further examination by SAED and by high-resolution TEM revealed that the sheath possesses an amorphous structure. A nano-sized electron beam EDX analysis revealed that the shell layer is composed of Sb only. This is further illustrated by the EELS analysis, with a nano-sized electron beam focused on the center and edge of the wires, respectively, as shown in Fig. 4. Checking with the EELS atlas, it is certain that the shell does not contain any indium. It is also not likely that the shell contains any oxygen, as the Sb $M_{4,5}$ has a pre-edge feature similar to what we have. An EELS of the Sb oxide is also shown in Fig. 4 as a reference to illustrate that the amorphous shell layer is not Sb oxide, but Sb.

The preparation of In_2O_3 nanowires by thermal evaporation methods has been widely reported and the mechanism of the processes has also been postulated. Most of the processes that use a catalyst were explained in terms of the vapor–liquid–solid (VLS) mechanism. In previous reports,

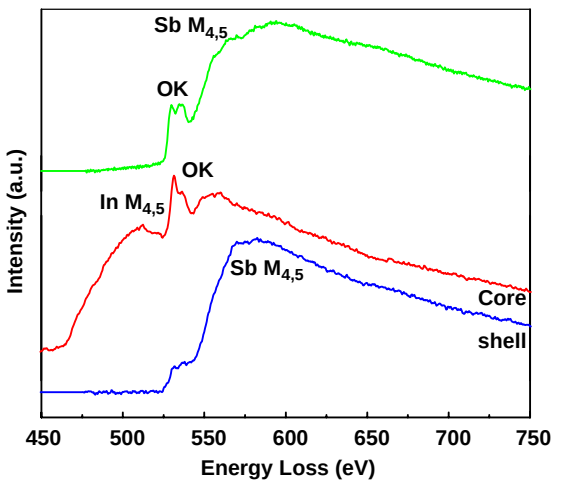

Fig. 4. EELS of the In_2O_3 nanowires from the core region, outside amorphous layer, and a reference Sb oxide.

the product area was somewhat remote from the source area, and the temperature in source area was usually above 800 °C and much higher than that in the cold product area. A process to transport vapors from the hot area to the cold area is necessary. In our experiment, the situation is quite different because the whole synthesis process happened in situ directly. An explanation of the nanowire growth mechanism must remain speculative. In the reaction process, the In liquid should be formed first because of its low-melting point; then, the oxygen dissolves into the liquid. After the In alloy is saturated with oxygen, the In_2O_3 will form. Some Sb may also dissolve into the In alloy, especially in the interface area between the Sb and In. But it is impossible to form Sb_2O_3 at such low temperatures, because the Gibbs energy of formation ($\Delta G^\circ_{f,540\,K}$) of Sb_2O_3 ($-485.11\,kJ\,mol^{-1}$) is much smaller than that of In_2O_3($-669.6\,kJ\,mol^{-1}$) [21]. However, we found that the existence of Sb was essential to obtain In_2O_3 nanowires at a low temperature of 540 °C. Without the presence of Sb, no In_2O_3 nanowire formed at this temperature. Furthermore, we have observed that some of the nanowire tips contain mainly Sb. Therefore; we believe that Sb acts as a catalyst to direct the growth of the In_2O_3 nanowires through a VLS growth mechanism. The residual oxygen gas inside the tube furnace provides the necessary oxygen for the formation of In_2O_3 nanowires. Due to the insufficient amount of oxygen, Sb is not oxidized and forms into an amorphous structure outside the In_2O_3 nanowires, and acts as surfactant to confine the size of the In_2O_3 nanowires to prevent them from growing laterally. It is suggested that the growth mechanism of the In_2O_3/Sb nanostructures is determined by the following factors: (1) the catalytic effect of the Sb sheath on the nanowire tips; and (2) the {1 0 0} surface, which has the lowest surface energy among the In_2O_3 surfaces and plays an important role during the nanowire growth. Since the surface energy is more important when the crystal size is reduced to nanoscale, it is believed that the absorbance of the Sb layer can reduce the system energy.

Fig. 5(a) is a typical HRTEM image of the surface of an In_2O_3 nanowire showing that the

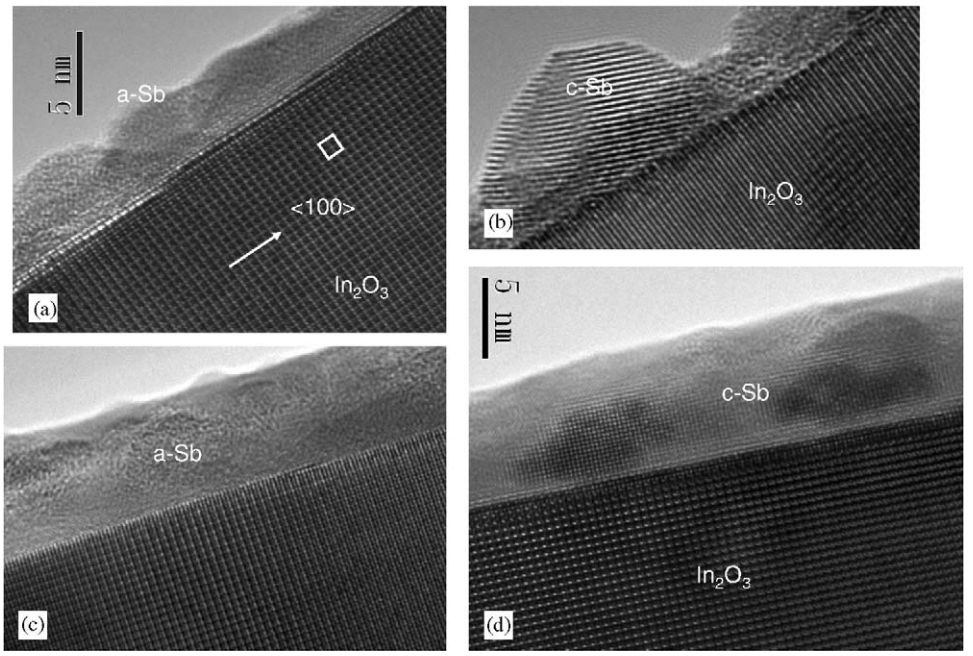

Fig. 5. HREM images of the In_2O_3 nanowires: (a) and (c) are the images at the initial state, (b) and (d) are the images after more than 10 min. of focused electron beam irradiation. The observation direction is along [0 0 1] of In_2O_3, and the outlined square in (a) illustrates a unit cell of In_2O_3 lattice.

In_2O_3 nanowires grow along the ⟨1 0 0⟩ direction with a single-crystalline nature, and that the surface of the wire is parallel to {1 0 0} planes. It is apparent that an atomic layer of steps is usually present at the surface. The presence of a large amount of atomic steps, and their accumulation, provides nucleation for the rectangular turning of the In_2O_3 nanowires. A round rectangular turning matches this explanation. The Sb shell layer of the In_2O_3 nanowire is in an amorphous structure, and it is interesting to be noted that, under the irradiation of an electron beam for more than 10 min, this amorphous layer gradually crystallized as shown in Fig. 5(b). A large number of experiments revealed that the crystallized Sb can be cataloged into a face center cubic (fcc) structure with a lattice constant of around 0.55 nm. An epitaxial relationship can be identified in some of the crystallized Sb with the In_2O_3 core structure. Figs. 5(c) and (d) are HRTEM images of another area showing that the amorphous structure changes to a crystalline structure with an epitaxial relationship with In_2O_3, i.e., (1 0 0)In_2O_3//(1 0 0)Sb and [0 0 1]In_2O_3///[0 0 1]Sb. It has been reported that amorphous Sb film can easily form by low-energy cluster beam deposition or by vacuum evaporation [22,23], and some results regarding the crystal growth have been achieved. Concerning the activation energy for crystal growth in amorphous films, values from 0.32 to 0.55 eV have been obtained, depending on the thickness of the film [24]. However, few studies have been conducted on the crystallization of nanometer-sized particles. Here, the crystallization of Sb during the electron irradiation can be understood from a thermodynamic point of view. The crystallization of Sb under electron beam irradiation is thought to be due to the electron beam-induced heating effect. However, when the growth temperature was increased, the amorphous Sb outside the In_2O_3 nanowires evaporated, leaving the In_2O_3 nanowires with a reasonable clean surface. Therefore, we conclude that the crystallization of the amorphous Sb sheath is induced by electron beam irradiation instead a thermal effect. The epitaxial relationship between the crystallized Sb and In_2O_3 indicates that the surfaces of In_2O_3 provide the nucleation sites and determine the crystalline

orientations of Sb. Therefore, the existence of an epitaxial relationship between the crystallized Sb and In_2O_3 provides a possibility to make a core-shell cable structure containing the Sb nanotubes surrounding the In_2O_3 nanowires. Sb is a semimetal containing electron and holes as charge carriers, and also a good superconductor material. The core-shell structure of In_2O_3/Sb provides a junction between the oxide semiconductor and semimetal, and may find its application in the fabrication of nanodevices.

4. Conclusion

The mass product of the In_2O_3/Sb core-shell cable-like nanostructures was synthesized by a thermal evaporation method by co-evaporating In and Sb catalyst at 540 °C. The nanowires present a rectangular turning feature with typical morphologies of "L," "T," and "H" shapes, and amorphous Sb shell layers around the In_2O_3 nanowires forming co-axis structures. Under focused electron beam irradiation, the amorphous Sb layer crystallized into a cubic structure. An epitaxial relationship was found to exist between the crystallized Sb and In_2O_3.

Acknowledgments

This work was supported by a Postdoctoral Fellow project of the Hong Kong Polytechnic University (G-YX17). One of the author (C.W. Lai) is supported by a graduated studentship of the Hong Kong Polytechnic University.

References

[1] S. Iijima, Nature 354 (1991) 56.
[2] M.H. Dvoret, D. Esteve, C. Urbina, Nature 360 (1992) 547.
[3] H. Dai, E.W. Wong, Y.Z. Lu, S. Fan, C.M. Lieber, Nature 375 (1995) 769.
[4] A.M. Morales, Lieber, Science 279 (1998) 208.
[5] Y. Zhang, K. Suenaga, C. Colliex, S. Iijima, Science 281 (1998) 973.
[6] K. Suenaga, C. Colliex, N. Demoncy, A. Loiseau, H. Pascard, F. Willaime, Science 278 (1997) 653.
[7] Y. Li, Y. Bando, D. Golberg, Adv. Mater. 16 (2004) 93.
[8] Dai Hau Zhang, et al., Nano Lett. 4 (2004) 1919.
[9] Chao Li, et al., Appl. Phys. Lett. 82 (2003) 1613.
[10] C. Chao Li, et al., Adv. Mater 15 (2003) 143.
[11] Pho Nguyen, et al., Nano Lett. 4 (2004) 651.
[12] J.S. Jeong, et al., Chem. Phys. Lett. 384 (2004) 246.
[13] C.H. Liang, et al., Adv. Mater. 13 (2001) 1330.
[14] Fanhao Zeng, et al., Nanotechnology 15 (2004) 596.
[15] P. Guha, S. Kar, S. Chaudhuri, Appl. Phys. Lett. 85 (2004) 3851.
[16] Yubao Li, Yoshio Bando, Dmitri Golberg, Adv. Mater. 15 (2003) 581.
[17] X.C. Wu, et al., Chem. Phys.Lett. 373 (2003) 28.
[18] X.F. Chu, et al., Chem. Phys.Lett. 399 (2003) 461.
[19] Maojun Zheng, et al., Appl. Phys. Lett. 79 (2001) 839.
[20] Maojun Zheng, et al., Chem. Phys Lett. 334 (2001) 298.
[21] J.A. Dean, Lange's Handbook of Chemistry, 14th ed, McGraw-Hill, Inc., New York, 1992, p. 6.71.
[22] H. Mori, M. Hashimoto, Thin Solid Films 205 (1991) 29.
[23] P. Jensen, P. Melinon, et al., Appl. Phys. Lett. 59 (1991) 16.
[24] M. Hashimoto, T. Niizeki, K. Kambe, Jpn. Appl. Phys. 19 (1980) 21.